Astron. Astrophys. 329, 754–764 (1998)

ASTRONOMY
AND
ASTROPHYSICS

Wave heating of coronal arcades driven by toroidally polarised footpoint motions

Stationary behaviour in dissipative MHD

W.J. Tirry⋆ **and S. Poedts**⋆⋆

Centre for Plasma Astrophysics, K.U. Leuven, Celestijnenlaan 200 B, B-3001 Heverlee, Belgium

Received 9 June 1997 / Accepted 21 August 1997

Abstract. We study the heating of 2-D coronal arcades by linear resonant Alfvén waves that are excited by photospheric footpoint motions of the magnetic field lines. The analysis is restricted to toroidally polarised footpoint motions so that Alfvén waves are excited directly. At the magnetic surfaces where Alfvén waves, travelling back and forth along the loop-like magnetic field lines, are in phase with the footpoint motions, the oscillations grow unbounded in ideal linear MHD. Inclusion of dissipation prevents singular growth and we can look at the steady state in which the energy input at the photospheric base of the arcade is balanced by the energy dissipated at the resonance layer.

In the present study we take the toroidal wave number to be non-zero which means that also fast waves, including quasi-modes, can be excited by the purely toroidally polarised footpoint motions. In this case resonant Alfvén waves are not only excited directly by the footpoint motions but also indirectly through coupling to the fast waves. Our results confirm the phenomena previous found by Berghmans & Tirry (1997) for a coronal loop model : for some footpoint motions the direct and indirect contributions to the resonance counteract each other leading to virtually no heating (anti-resonance) while, for values of the driving frequency and the toroidal wave number corresponding to a quasi-mode, the two contributions act in concert leading to enhanced heating.

Key words: MHD – Sun: corona – Sun: magnetic fields-waves – methods: analytical; numerical

1. Introduction

The solar corona consists of highly inhomogeneous plasma with a temperature of roughly $2 - 3 \times 10^6$ K. This temperature is a few orders higher than the underlying photospheric temperature, indicating the presence of heating mechanisms. Since Skylab it is known that the largest contribution to the X-ray emission and to the heating of the solar corona comes from loop-like structures in the solar atmosphere. These magnetic loops and arcade structures are viewed as the basic building blocks of the solar corona. For example, Acton et al. (1992) show an X-ray image in which a magnetic arcade is present with following length scales : half a solar radius high, 400,000 km wide and 500,000 km long. A large variety of similar structures, with various heights, widths and lengths, can be seen in many Yohkoh pictures (McAllister et al. 1992; Watari et al. 1996; Weiss et al. 1996).

The high conductivity and the relatively high mass density of the photospheric plasma provide an effective photospheric anchoring of the magnetic field lines. The photospheric footpoints of the magnetic field lines are forced to follow the convective motions. If these footpoint motions are slow (in comparison with the Alfvénic transit time along the loop or arcade), the coronal flux tubes are twisted and braided, which builds up magnetic stresses and leads to the formation of small length scale by the creation of field discontinuities (Parker 1972) or by cascade of magnetic energy to very small length scales (Van Ballegooijen 1985). These mechanisms to generate small length scales, and hence heating, are usually classified as DC heating mechanisms (Zirker 1993).

In contrast, footpoint motions which are 'fast' in comparison with the Alfvénic transit time, generate magnetosonic waves and Alfvén waves. Due to the steep density gradients at the photospheric edges these MHD waves reflect back and forth along the length of the loop. The loop is then expected to act as a leaking, resonant cavity for MHD waves (Hollweg 1984), in which dissipation is enhanced by means of turbulence, resonant absorption and/or phase-mixing. These mechanisms are classified as AC heating mechanisms.

Observations suggest that periodic and quasi-periodic oscillations commonly occur in the corona. Oscillations are detected by measuring the temporal variation in intensity, line width and Doppler velocity of coronal emission lines. A thor-

Send offprint requests to: W.J. Tirry

⋆ Research Assistant of the F.W.O.-Vlaanderen

⋆⋆ Research Associate of the F.W.O.-Vlaanderen

ough review of this observational background can be found in Tsubaki (1988). Many of the observed periods are of the order of five minutes understood as an evidence of the propagation of the 5-min oscillation into the chromosphere and corona. Pasachoff & Landman (1984), Pasachoff & Ladd (1987) and Pasachoff (1991) however detected intensity variations of the green coronal line with enhanced power in the 0.25-2 Hz range. Recent studies of soft X-ray lines indicate nonthermal motions of 30-40 km/s above active regions (Saba & Strong 1991).

Recent observations by Falconer et al. (1996) suggest that the different heating mechanisms may co-operate : microflaring in the chromospheric magnetic network might both directly heat the coronal plasma in the sheared local core field and generate waves that propagate into extended loops and dissipate there to produce the enhanced coronal heating in the bodies of these larger structures.

An important property of MHD waves in an inhomogeneous plasma is that individual magnetic surfaces can oscillate with their own Alfvén frequencies. In ideal linear MHD this can happen without interaction with neighbouring magnetic surfaces. These local Alfvén oscillations are polarised in the magnetic surfaces and perpendicular to the magnetic field lines. Dissipative effects produce coupling to neighbouring surfaces. For large values of the viscous and magnetic Reynolds numbers, such as in the solar corona the local Alfvén oscillations are still characterized by steep gradients across the magnetic surfaces. Resonant excitation of these local Alfvén oscillations provides a way to dissipate wave energy efficiently.

Berghmans & Tirry (1997) studied the heating of 1-D coronal loops by these linear resonant Alfvén waves that are excited by photospheric footpoint motions of the magnetic field lines. The analysis was restricted to azimuthally polarised footpoint motions so that Alfvén waves are excited directly. At the radii where Alfvén waves, travelling back and forth along the loop, are in phase with the footpoint motions the oscillations grow unbounded in ideal MHD. They included dissipation and looked at the steady state in which the energy input at the photosphere is balanced by the energy dissipated at the resonance. In contrast to previous studies on this subject (Heyvaerts & Priest 1983; Berghmans & De Bruyne 1995; Poedts & Boynton 1996; Ruderman et al. 1997a) the toroidal wave number was taken to be non-zero which means that also fast waves, including quasi-modes, can be excited by the purely toroidally polarised footpoint motions. In this case resonant Alfvén waves are not only excited directly by the footpoint motions but also indirectly through coupling to fast waves. Berghmans & Tirry found that for some footpoint motions these contributions counteract each other leading to virtually no heating (anti-resonance) while for values of the driving frequency and the azimuthal wave number corresponding to a quasi-mode the two contributions act in concert leading to enhanced heating. These results were confirmed in a companion paper (Tirry & Berghmans 1997) where the same system was studied time dependently in linear ideal MHD.

Ruderman et al. (1997b) extended the analysis to 2-D coronal arcades driven by footpoint motions, however with the toroidal wave number equal to zero so that no coupling to fast waves is involved.

The main objective of this paper is to extend the above mentioned investigations of wave heating to 2-D coronal arcades where the toroidal wave number is taken non-zero and to find out whether the anti-resonance line in (ω_d, k_y) space found by Berghmans & Tirry (1997) is not an artefact of their 1-D coronal loop model.

Few authors already have explored the modes of oscillation of coronal magnetic arcade structures. Poedts & Goossens (1991) have studied the continuous spectrum in linear ideal MHD of 2-D solar loops and arcades in different cases. Oliver et al. (1993, 1996) investigated the magnetoacoustic modes of potential and non-potential coronal arcades. By looking at the perturbed restoring forces responsible for the oscillatory modes they could still classify the modes as modes with fast wave properties or with slow wave properties. Čadež & Ballester (1996) considered an isolated isothermal potential arcade with a thick boundary layer of non-potential magnetic field. For large enough wavelengths surface waves on this structure may resonantly couple to localised slow modes. Smith et al. (1997) examined the effect of curvature on fast magnetoacoustic waves in dense coronal loops situated in a potential coronal arcade. Čadež & Ballester (1995a,b) obtained analytically the time-dependent solution for fast magnetoacoustic waves generated by a distinct periodic perturber or impulsively excited by a localised perturber in a potential coronal arcade.

The present paper is organized as follows. In the next section the coronal arcade model, the relevant equations, the boundary conditions and the underlying assumptions are discussed. In Sect. 3 we derive an analytical solution which describes the wave motion in the dissipative layer embracing the resonant magnetic surface. We describe shortly in Sect. 4 the numerical procedure to find the steady state solution, in which we use the analytical solution from Sect. 3 to cross the dissipative resonance layers while integrating the ideal MHD equations. In Sect. 5 we derive an expression for the Poynting flux through the photosphere as a function of the steady state wave amplitude. This turns out to be a valuable tool when interpreting the results in Sect. 6. Finally in Sect. 7 we give a summary and discussion.

2. Physical model

We consider a two-dimensional (x, z) coronal arcade with width $2L$ which is invariant in the y-direction, modelled with a potential equilibrium magnetic field satisfying

$$\nabla \times \boldsymbol{B} = 0 \quad \text{and} \quad B_y = 0,$$

i.e. the toroidal component of the magnetic field vanishes. From the solenoidal constraint $\nabla \cdot \boldsymbol{B} = 0$, the poloidal equilibrium magnetic field $\boldsymbol{B}$ can be written as

$$\boldsymbol{B} = \nabla \times \psi(x, z)\hat{e}_y,$$

where the magnetic flux function ψ satisfies $\nabla^2\psi = 0$. Under the conditions that ψ vanishes at infinite height and that the z-component of the magnetic field is zero at the centre ($x = 0$) of

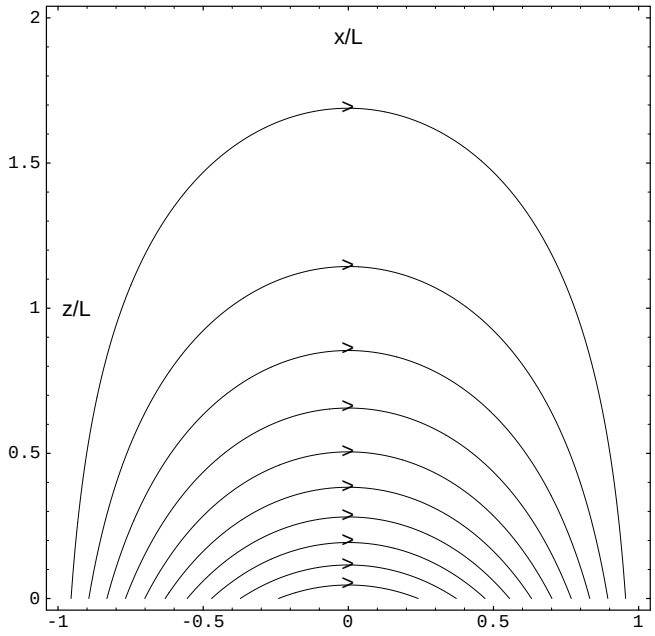

Fig. 1. The form of the potential coronal arcade in the cartesian coordinates (x, z).

the arcade, the following particular solution for the flux function is taken

$$\psi(x,z) = B_0\lambda_B \cos(\frac{x}{\lambda_B})\exp(\frac{-z}{\lambda_B}), \tag{1}$$

where B_0 is the magnetic field strength at the base $z = 0$ of the corona and $\lambda_B = 2L/\pi$ is the magnetic scale height. The magnetic surfaces are given by $\psi(x, z) = \text{const}$. Fig. 1 shows the form of the potential coronal arcade in the (x, z) plane. The surface $z = 0$ models the boundary between the hot rarified corona and the dense photosphere. We assume that the magnetic field lines are frozen into the highly dense photosphere.

We consider small amplitude motions of a resistive plasma which can be described by the linearized gravitationless MHD equations

$$\rho\frac{\partial^2\boldsymbol{\xi}}{\partial t^2} = \frac{1}{\mu}(\nabla\times\boldsymbol{b})\times\boldsymbol{B}, \tag{2}$$

$$\frac{\partial\boldsymbol{b}}{\partial t} = \nabla\times(\frac{\partial\boldsymbol{\xi}}{\partial t}\times\boldsymbol{B}) - \nabla\times(\eta\nabla\times\boldsymbol{b}), \tag{3}$$

where $\boldsymbol{\xi}$ is the Lagrangian displacement and $\boldsymbol{b}$ the magnetic field perturbation. The gas pressure is neglected in comparison with the magnetic pressure in the zero-β approximation for the solar corona. Although we did not include the gravity force in the momentum equation (because of the extreme low density in the solar corona), density stratification is taken into account (see expression (13)). The spatial dependence of the magnetic diffusivity η will be specified later on the basis of mathematical tractability.

Now we introduce the function $\chi(x, z)$ which satifies the equation

$$\frac{\partial\chi}{\partial x}\frac{\partial\psi}{\partial x} + \frac{\partial\chi}{\partial z}\frac{\partial\psi}{\partial z} = 0.$$

Hence the function χ and ψ constitute an orthogonal curvilinear coordinate system in the (x, z) plane. For the flux function ψ given by (1), the function χ can be taken to be

$$\chi(x,z) = B_0\lambda_B \sin(\frac{x}{\lambda_B})\exp(\frac{-z}{\lambda_B}). \tag{4}$$

At the left footpoint of the magnetic surface $\psi = \text{const}$ the poloidal coordinate χ takes the value $\chi_1(\psi)$, while at the right footpoint it takes the value $\chi_2(\psi)$. At $\chi = \chi_1(\psi)$ we impose a given footpoint motion whereas at $\chi = \chi_2(\psi)$ we assume the arcade to be held immovable. This can be done without any loss of generality because of the principle of superposition for solutions of linear equations. For the present paper in which we focus on excitation by toroidally polarised footpoint motions (i.e. in the y-direction), this means that we impose the following boundary conditions at $\chi = \chi_1$:

$$\begin{aligned}
\xi_\chi(\chi = \chi_1(\psi), \psi, y, t) &= 0,\\
\xi_\psi(\chi = \chi_1(\psi), \psi, y, t) &= 0,\\
\xi_y(\chi = \chi_1(\psi), \psi, y, t) &= R_y(\psi, y, t),
\end{aligned}$$

and at $\chi = \chi_2$ (for this symmetric model $\chi_2 = -\chi_1$) :

$$\begin{aligned}
\xi_\chi(\chi = \chi_2(\psi), \psi, y, t) &= 0,\\
\xi_\psi(\chi = \chi_2(\psi), \psi, y, t) &= 0,\\
\xi_y(\chi = \chi_2(\psi), \psi, y, t) &= 0.
\end{aligned}$$

Since we consider only the steady state of the driven oscillations, the perturbed quantities are taken to be proportional to $\exp(-i\omega t)$ with real ω given. Because the equilibrium state is invariant in the y-direction, we can Fourier analyse with respect to y and study the Fourier components corresponding to different k_y separately (as they do not couple).

For high magnetic Reynolds numbers such as in the solar corona, the ideal counterparts of Eqs. (2-3) are valid everywhere except in regions where the solution has steep gradients (e.g. in resonance layers). In these dissipative resonance layers gradients of perturbations in the ψ-direction are by far larger than gradients in the χ-direction. These considerations enable us to reduce the resistive equations for the Fourier component corresponding to the wave number k_y in the following form

$$\{\rho J\omega^2 + \frac{\partial}{\partial\chi}\frac{1}{J}\frac{\partial}{\partial\chi} - i\eta\omega\rho\frac{\partial^2}{\partial\psi^2}\}\xi_y = ik_yP, \tag{5}$$

$$\{\rho J\omega^2 + \frac{1}{J}\frac{\partial^2}{\partial\chi^2} - i\eta\omega\rho\frac{\partial^2}{\partial\psi^2}\}\bar{\xi}_\psi = \frac{1}{J}\frac{\partial P}{\partial\psi}, \tag{6}$$

$$P = -\frac{\partial\bar{\xi}_\psi}{\partial\psi} - ik_y\xi_y, \tag{7}$$

where $P = JB_\chi b_\chi$, $\bar{\xi}_\psi = B_\chi\xi_\psi$ and J is the jacobian of the transformation. For mathematical tractability we have assumed

in the derivation of Eqs. (5) and (6) that the quantity η/J is a constant. Note that slow waves are absent ($\xi_\chi = 0$) because the plasma pressure is neglected.

In order to get homogeneous boundary conditions we introduce a new variable

$$\phi(\chi,\psi) = \xi_y(\chi,\psi) - \frac{\chi-\chi_2(\psi)}{\chi_1(\psi)-\chi_2(\psi)} R_y(\psi). \tag{8}$$

Substituting (8) into (5-7) we obtain under the condition that the characteristic scale of the variation of the driver is much larger than the thickness of the dissipative layer :

$$\{\rho J\omega^2 + \frac{\partial}{\partial\chi}\frac{1}{J}\frac{\partial}{\partial\chi} - i\eta\omega\rho\frac{\partial^2}{\partial\psi^2}\}\phi = ik_y P' + D_y, \tag{9}$$

$$\{\rho J\omega^2 + \frac{1}{J}\frac{\partial^2}{\partial\chi^2} - i\eta\omega\rho\frac{\partial^2}{\partial\psi^2}\}\bar{\xi}_\psi = \frac{1}{J}\frac{\partial P'}{\partial\psi} + D_\psi, \tag{10}$$

$$P' = -\frac{\partial\bar{\xi}_\psi}{\partial\psi} - ik_y\phi, \tag{11}$$

where

$$\begin{aligned} D_y(\chi,\psi) &= \frac{\chi-\chi_2}{\chi_1-\chi_2}(k_y^2-\rho J\omega^2)R_y \\ &\quad -\frac{\partial}{\partial\chi}\left(\frac{1}{J}\frac{\partial}{\partial\chi}\left(\frac{\chi-\chi_2}{\chi_1-\chi_2}\right)\right)R_y, \\ D_\psi(\chi,\psi) &= -\frac{ik_y}{J}\frac{\partial}{\partial\psi}\left(\left(\frac{\chi-\chi_2}{\chi_1-\chi_2}\right)R_y\right). \end{aligned}$$

Since we have neglected the pressure and gravity terms in the momentum equation, we are able to impose the density or the Alfvén speed profile arbitrarily. Oliver et al. (1993) investigated the normal modes of the present magnetic structure for a variety of density profiles and found that whenever the Alfvén speed decreases or remains constant with height, the solutions for ξ_ψ diverge as z tends to infinity. Therefore we choose a $v_A(x,z)$ that exponentially increases with height, taking

$$v_A(x,z) = v_{A0}\exp(\frac{z}{2\lambda_B}), \tag{12}$$

where v_{A0} is the Alfvén speed at the base of the coronal arcade. The density is then determined by (1) and (12) as

$$\rho(x,z) = \rho_0\exp(\frac{-3z}{\lambda_B}). \tag{13}$$

For the rest of the paper length, speed, density and magnetic field strength are non-dimensionalized with respect to λ_B, v_{A0}, ρ_0 and B_0 respectively.

3. Analytical solution

Eqs. (9-11) show that, when $k_y = 0$, the Alfvén (ξ_y component) and fast (ξ_ψ component) waves are decoupled. Hence when the footpoint motions are purely toroidal, only Alfvén waves are generated and propagate along the magnetic field lines with the local Alfvén speed. As the local Alfvén speed varies across the magnetic surfaces (and along the magnetic field lines), the Alfvén waves on different surfaces become out of phase. This phase-mixing creates small length scales necessary for dissipation to become effective in the solar corona.

Due to the high conductivity and the relatively high mass density of the photosphere the Alfvén waves reflect back and forth along the length of the arcade at the photospheric edges. When the driving frequency matches the local Alfvén eigenfrequency, a resonance is built up. In ideal MHD the amplitude at the resonant magnetic surface grows linearly in time. On the non-resonant surfaces beat phenomena are seen (Berghmans & De Bruyne 1995). Ruderman et al. (1997b) included viscosity and resistivity and looked at the steady state solution in which the energy input at the photosphere is balanced by the energy dissipated at the resonance layer. They found that the distribution of the dissipated energy along the dissipative layer strongly depends on the ratio of the viscosity and the resistivity. However the total amount of dissipated energy is independent of this ratio.

When $k_y \neq 0$, the Alfvén and fast waves do not exist any longer independently. The purely toroidal footpoint motions now also generates indirectly a ξ_ψ component through coupling with the directly excited ξ_y component. Since this coupling has its influence on the resonantly excited Alfvén waves, it is instructive, not only to examine the Alfvén wave spectrum but also the fast mode spectrum. This is done in the following first subsection.

In the second subsection we derive an analytical solution in the dissipative layer around the resonant magnetic surface, so that the required numerical effort to find the steady state solution is limited to the integration of the ideal MHD equations in regions away from any singularity. Hence this approach saves a lot of memory and CPU time, and allows for a straightforward parametric study.

3.1. The eigenvalue problem

For $R_y = 0$ and $k_y = 0$ Eqs. (9-11) form two separate eigenvalue problems for the Alfvén and fast modes. The fast magnetosonic spectrum is governed by

$$\{\rho J\omega^2 + \frac{1}{J}\frac{\partial^2}{\partial\chi^2} + \frac{1}{J}\frac{\partial^2}{\partial\psi^2}\}\bar{\xi}_\psi = 0,$$

supplied with the necessary boundary conditions in χ and ψ. The effects of curvature (present in the jacobian $1/J$) on these fast magnetoacoustic eigenmodes are, for example, studied by Smith et al. (1997) for dense coronal loops situated in the potential arcade. On the other hand, the Alfvén spectrum is governed by

$$\{\rho J\omega^2 + \frac{\partial}{\partial\chi}\frac{1}{J}\frac{\partial}{\partial\chi}\}\xi_y = 0.$$

Here ψ shows up as a parameter in the equation : for each value of ψ the equation forms a Sturm Liouville eigenvalue problem. When one varies ψ the corresponding discrete spectrum $\{\omega_A^{(n)}(\psi)\}$ is smeared out in a discrete set of continua. For every

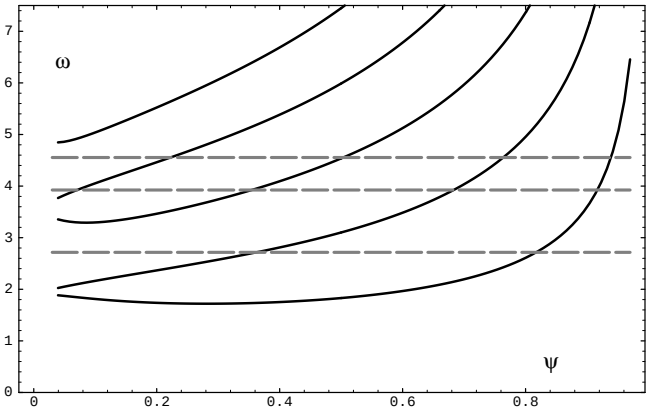

Fig. 2. The first 5 Alfvén continua together with the first 3 fast mode eigenfrequencies (indicated as horizontal gray dashed lines).

fixed ψ_0 the corresponding eigenfunctions $\{w_n(\chi,\psi_0)\}$ constitute a complete orthonormal set of functions in the interval $\chi_1(\psi_0) \leq \chi \leq \chi_2(\psi_0)$. The Alfvén eigenfunctions are orthonormal in the sense that

$$\langle w_n \rho J w_{n'} \rangle = \int_{\chi_1}^{\chi_2} w_n \rho J w_{n'} \mathrm{d}\chi = \delta_{nn'}. \tag{14}$$

Since the potential arcade is symmetric with respect to $\chi = 0$, the eigenfunctions (for both the fast as the Alfvén spectrum) split up in a set of even functions and a set of odd functions with respect to $\chi = 0$. Fig. 2 shows the first 5 Alfvén continua together with the first three fast mode eigenfrequencies (which are indicated in the picture as horizontal gray dashed lines).

For the case that $k_y \neq 0$ the Alfvén and fast modes do not exist any longer independently. At certain magnetic surfaces the fast mode can be resonantly coupled to local Alfvén waves. Hence the corresponding eigenvalue problem transforms into the eigenvalue problem for the quasi-modes (see e.g. Tirry & Goossens 1996).

3.2. Solution in the resonance layer

Since the Alfvén eigenfunctions form a complete orthonormal set of functions in the interval $\chi_1(\psi) \leq \chi \leq \chi_2(\psi)$, it is convenient to expand ϕ, $\bar{\xi}_\psi$ and P' with respect to the eigenfunctions $\{w_n(\chi,\psi)\}$:

$$\phi(\chi,\psi) = \sum_{n=1}^{\infty} Y_n(\psi) w_n(\chi,\psi),$$

$$\bar{\xi}_\psi(\chi,\psi) = \sum_{n=1}^{\infty} X_n(\psi) w_n(\chi,\psi),$$

$$P'(\chi,\psi) = \sum_{n=1}^{\infty} P_n(\psi) w_n(\chi,\psi).$$

Substituting these expansions into the ideal counterparts of (9-11) and using the orthonormality relationship (14), we get for each n :

$$(\omega^2 - \omega_A^{(n)2}) Y_n = i k_y \sum_{m=1}^{\infty} P_m \langle w_m w_n \rangle + \langle D_y w_n \rangle, \tag{15}$$

$$\omega^2 X_n + \sum_{m=1}^{\infty} X_m \langle \frac{1}{J} \frac{\partial^2 w_m}{\partial \chi^2} w_n \rangle = \sum_{m=1}^{\infty} \{ \frac{\partial P_m}{\partial \psi} \langle \frac{1}{J} w_m w_n \rangle + P_m \langle \frac{1}{J} \frac{\partial w_m}{\partial \psi} w_n \rangle \} + \langle D_\psi w_n \rangle, \tag{16}$$

$$P_n = -\frac{\partial X_n}{\partial \psi} - \sum_{m=1}^{\infty} X_m \langle \rho J \frac{\partial w_m}{\partial \psi} w_n \rangle - i k_y Y_n. \tag{17}$$

After truncating the series at certain value of m this set of equations can easily be integrated numerically, unless a singularity is encountered. From Eq. (15) we see that a singularity occurs at the magnetic surface where the driving frequency ω equals the local Alfvén frequency $\omega_A^{(n)}$. In what follows we assume that the resonance occurs at $\psi = \psi_A$ for $n = r$.

First of all, when we substitute Eq. (11) into (10) and use the fact that in the dissipative layer gradients of ξ_ψ in the ψ-direction are by far larger than gradients in the χ-direction, we can deduce that P' (related to the magnetic pressure) varies approximately linearly across the resonant magnetic surface $\psi = \psi_A$:

$$P' \approx P^A(\chi) + J(\chi,\psi_A) D_\psi(\chi,\psi_A)(\psi - \psi_A).$$

This results enables us to approximate the solution close to the resonance for Y_n with $n \neq r$ as

$$Y_n = \frac{1}{\omega^2 - \omega_A^{(n)2}} \{ i k_y \sum_{m=1}^{\infty} P_m^A \langle w_m w_n \rangle + i k_y \langle J D_\psi w_n \rangle (\psi - \psi_A) + \langle D_y w_n \rangle \}. \tag{18}$$

However for the resonant harmonic $Y_r(\psi)$ the inversion as in Eq. (18) is not possible : dissipation is important in the resonance layer and thus the resistive term in Eq. (9) has to be included. In the dissipative layer we can make the following approximation for the resonant harmonic :

$$\frac{\partial^2}{\partial \psi^2}(Y_r w_r) \approx w_r \frac{\partial^2 Y_r}{\partial \psi^2}.$$

Hence the resistive counterpart of Eq. (15) for the resonant harmonic Y_r yields close to the resonant magnetic surface

$$\{ (\omega^2 - \omega_A^{(r)2}(\psi)) - i \frac{\eta \omega}{J} \frac{\partial^2}{\partial \psi^2} \} Y_r = i k_y \sum_{m=1}^{\infty} P_m^A \langle w_m w_r \rangle + \langle D_y w_r \rangle. \tag{19}$$

Now we define s_A such that $\omega^2 - \omega_A^{(r)2}(\psi)$ can be represented in the interval $[\psi_A - s_A, \psi_A + s_A]$ by the first term of the Taylor expansion :

$$\omega^2 - \omega_A^{(r)2}(\psi) = \Delta(\psi - \psi_A), \tag{20}$$

where

$$\Delta = \frac{d}{d\psi}(\omega^2 - \omega_A^{(r)2})|_{\psi=\psi_A}.$$

In Eq. (19) the highest derivative term is multiplied with the magnetic diffusivity. Thus, for very high Reynolds numbers Eq. (19) represents a singular perturbation problem. Dissipation is only important in a thin layer embracing the resonant magnetic surface where the first term in the lefthandside of Eq. (19) is of the order of the second term. Comparison of these two terms results in a thickness of the dissipative layer δ_A given by

$$\delta_A = (\frac{\omega\eta}{J|\Delta|})^{\frac{1}{3}}.$$

Due to the very large Reynolds numbers in the solar corona, the thickness of the resonant layer δ_A is in general much smaller than the range of validity of the Taylor expansion (20). This is important since it implies that in addition to the dissipative layer there are two overlap regions to the left and the right of the dissipative layer contained in the interval $[\psi_A - s_A, \psi_A + s_A]$ where ideal MHD is valid too.

Then it is convenient to introduce a new scaled variable $\tau = (\psi - \psi_A)/\delta_A$ which is of the order 1 in the dissipative layer. In this new variable Eq. (19) transforms to

$$\{\frac{d^2}{d\tau^2} + i\text{sign}(\Delta)\tau\}Y_r = \frac{i}{\delta_A|\Delta|}\{ik_y\sum_{m=1}^{\infty}P_m^A\langle w_m w_r\rangle + \langle D_y w_r\rangle\}. \quad (21)$$

The solution to this equation which is bounded as $|\tau| \to \infty$ is given by (see e.g. Goossens, Ruderman & Hollweg 1995)

$$Y_r = \frac{-iF(\tau)}{\delta_A|\Delta|}\{ik_y\sum_{m=1}^{\infty}P_m^A\langle w_m w_r\rangle + \langle D_y w_r\rangle\} \quad (22)$$

where $F(\tau)$ is the universal function which was first introduced by Boris (1968)

$$F(\tau) = \int_0^{\infty}\exp(i\tau\text{sign}(\Delta)k - \frac{k^3}{3})\text{d}k.$$

From Eq. (17) the solution for the resonant harmonic in the expansions of $\bar{\xi}_\psi$ close to the resonant magnetic surface becomes

$$X_r = \frac{ik_y G(\tau)}{\Delta}(ik_y\sum_{m=1}^{\infty}P_m^A\langle w_m w_r\rangle + \langle D_y w_r\rangle) - P_r\delta_A\tau + C_X \quad (23)$$

where

$$G(\tau) = \int_0^{\infty}\exp(\frac{k^3}{3})\frac{\exp(i\tau\text{sign}(\Delta)k) - 1}{k}\text{d}k$$

and C_X is a constant of integration.

4. Numerical procedure

This section is devoted to a short description of the numerical approach to solve Eqs. (9-11) for ϕ, $\bar{\xi}_\psi$ and P'. Since in the orthogonal curvilinear coordinates (χ, ψ), as described in Sect. 2, the boundaries χ_1 and χ_2 are dependent on ψ, we prefer to transform to a new pair of flux coordinates, however non-orthogonal,

$$\begin{aligned}\psi' &= \psi; & 0 \le \psi' \le 1\\ \chi' &= (1-\psi^2)^{-\frac{1}{2}}\chi; & -1 \le \chi' \le 1\end{aligned}$$

With these coordinates, field lines become straight lines with ψ' = const and have length 2, which is achieved through the normalisation factor $(1-\psi^2)^{-\frac{1}{2}}$. The photosphere ($z = 0$) corresponds to $\chi' = 1$ for $0 \le x \le 1$ and to $\chi' = -1$ for $-1 \le x \le 0$. The line $\psi' = 0$ is the field line in the (x, z) system that originates at $(-L, 0)$, extending up to infinity and terminating at $(L, 0)$. The line $\psi' = 1$ corresponds to the point $(x = 0, z = 0)$ (Oliver et al. 1996).

The Eqs. (9-11) can be rewritten with these new flux coordinates into

$$\{\rho J\omega^2 + (1-\psi'^2)^{-1}\frac{\partial}{\partial\chi'}\frac{1}{J}\frac{\partial}{\partial\chi'} - i\eta\omega\rho\frac{\partial^2}{\partial\psi'^2}\}\phi = ik_y P' + D_y(\chi', \psi'), \quad (24)$$

$$\{\rho J\omega^2 + \frac{(1-\psi'^2)^{-1}}{J}\frac{\partial^2}{\partial\chi'^2} - i\eta\omega\rho\frac{\partial^2}{\partial\psi'^2}\}\bar{\xi}_\psi = \frac{1}{J}(\frac{\partial}{\partial\psi'} + \psi'(1-\psi'^2)^{-1}\chi'\frac{\partial}{\partial\chi'})P' + D_\psi(\chi', \psi'), \quad (25)$$

$$P' = -(\frac{\partial}{\partial\psi'} + \psi'(1-\psi'^2)^{-1}\chi'\frac{\partial}{\partial\chi'})\bar{\xi}_\psi - ik_y\phi, \quad (26)$$

where

$$\begin{aligned}D_y(\chi', \psi') &= \frac{1-\chi'}{2}(k_y^2 - \rho J\omega^2)R_y + \frac{(1-\psi'^2)^{-1}}{2}\frac{\partial}{\partial\chi'}(\frac{1}{J})R_y,\\ D_\psi(\chi', \psi') &= -\frac{ik_y}{J}\frac{1-\chi'}{2}\frac{\partial R_y}{\partial\psi'} + \frac{ik_y}{J}\psi'(1-\psi'^2)^{-1}\frac{\chi'}{2}R_y.\end{aligned}$$

At the coronal base $z = 0$ ($\chi' = \pm 1$) all the variables ϕ, $\bar{\xi}_\psi$ and P' should vanish. Remember that the footpoint motions are included as driving terms into the equations by (8). If we assume that the arcade under consideration is taken to be isolated in the sense that no plasma traverses the boundaries at $x = \pm L$ ($\psi' = 0$), $\bar{\xi}_\psi$ has to be zero at $\psi' = 0$.

The homogeneous boundary conditions for ϕ, $\bar{\xi}_\psi$ and P' at $\chi' = \pm 1$ allow for the following expansions

$$\phi(\chi', \psi') = \sum_{n=1}^{\infty}Y_n(\psi')w_{ne}(\chi', \psi'_e),$$

$$\bar{\xi}_\psi(\chi', \psi') = \sum_{n=1}^{\infty}X_n(\psi')w_{ne}(\chi', \psi'_e),$$

$$P'(\chi',\psi') = \sum_{n=1}^{\infty} P_n(\psi') w_{ne}(\chi',\psi'_e),$$

where $\{w_{ne}(\chi',\psi'_e)\}$ form the complete set of Alfvén eigenfunctions of the magnetic surface $\psi' = \psi'_e$. Note that, in contrast to the corresponding expansions in Sect. 3.2, the expansions are now with respect to the set of Alfvén eigenfunctions of one particular magnetic surface. This we can do because all field lines have the same length in the flux coordinates (χ',ψ'). For the numerics this means that we have to calculate the Alfvén eigenfunctions of only one magnetic surface. With the use of these expansions the ideal part of the coupled partial differential Eqs. (24-26) is replaced by an infinite set of coupled ODE's for X_n, Y_n and P_n. In contrast to a 1-D situation there is coupling between the different Alfvén eigenfunctions (see e.g. Tirry & Berghmans 1997) :

$$\omega^2 Y_n + \sum_{m=1}^{\infty} Y_m C1_{mn} - ik_y \sum_{m=1}^{\infty} P_m C2_{mn} = D1_n, \tag{27}$$

$$\omega^2 X_n + \sum_{m=1}^{\infty} X_m C3_{mn} - \sum_{m=1}^{\infty} \frac{\partial P_m}{\partial \psi'} C4_{mn} - \sum_{m=1}^{\infty} P_m C5_{mn} = D2_n, \tag{28}$$

$$P_n + ik_y Y_n + \frac{\partial X_n}{\partial \psi'} + \sum_{m=1}^{\infty} X_m C6_{mn} = 0 \tag{29}$$

with

$$\begin{aligned}
C1_{mn} &= \frac{1}{1-\psi'^2}\langle \frac{\rho_e J_e}{\rho J} \frac{\partial}{\partial \chi'}(\frac{1}{J}\frac{\partial w_{me}}{\partial \chi'}) w_{ne}\rangle \\
C2_{mn} &= \langle \frac{\rho_e J_e}{\rho J} w_{me} w_{ne}\rangle \\
C3_{mn} &= \frac{1}{1-\psi'^2}\langle \frac{\rho_e J_e}{\rho J^2} \frac{\partial w_{me}^2}{\partial \chi'^2} w_{ne}\rangle \\
C4_{mn} &= \langle \frac{\rho_e J_e}{\rho J^2} w_{me} w_{ne}\rangle \\
C5_{mn} &= \frac{\psi'}{1-\psi'^2}\langle \frac{\rho_e J_e}{\rho J^2} \chi' \frac{\partial w_{me}}{\partial \chi'} w_{ne}\rangle \\
C6_{mn} &= \frac{\psi'}{1-\psi'^2}\langle \rho_e J_e \chi' \frac{\partial w_{me}}{\partial \chi'} w_{ne}\rangle \\
D1_n &= \langle \frac{\rho_e J_e}{\rho J} D_y w_{ne}\rangle \\
D2_n &= \langle \frac{\rho_e J_e}{\rho J} D_\psi w_{ne}\rangle
\end{aligned}$$

where the subscript 'e' indicates that the quantities are evaluated at $\psi = \psi_e$. The ideal equations are then discretised using a finite differencing scheme (second order accuracy). After expanding the Alfvén eigenfunctions corresponding to a resonant magnetic surface $\psi' = \psi'_A$ with respect to $\{w_{ne}(\chi',\psi'_e)\}$ we can use the analytical solution (22-23) for the resonant variables to cross the dissipative layer embracing the resonant magnetic surface $\psi' = \psi'_A$. The non-resonant variables are linearly extrapolated across the resonance layer. The resulting linear algebraic equations are solved using standard NAGroutines.

5. Energetics

Once we have determined the stationary behaviour of the excited waves inside and outside the dissipative resonance layer we can study the resulting dissipation of the wave energy in the coronal arcade due to the resonance. In the steady state the energy, averaged over a period of the driving frequency, dissipated in the resonant layer must be balanced by the time-averaged energy that enters the arcade through the left foot of the arcade at $z = 0$. As the z-component of the velocity is equal to zero at $z = 0$, the time averaged energy flux through the left coronal base of the arcade is given by the z-component of the time averaged Poynting vector $\mathbf{E} \times \mathbf{B}^*$ integrated over this surface

$$S = \int_{-L}^{0} [\frac{Re(\mathbf{E} \times \mathbf{B}^*)_z}{2}]_{z=0} \, \mathrm{d}x, \tag{30}$$

where $Re(.)$ denotes the real part of a complex quantity, and the asterix its complex conjugate.

With the use of Ohm's law we easily get

$$\mathbf{E} \times \mathbf{B}^* = [\mathbf{v}|B|^2 - \mathbf{B}(\mathbf{v} \cdot \mathbf{B}^*)] + \eta(\nabla \times \mathbf{B}) \times \mathbf{B}^*. \tag{31}$$

Taking into account the fact that we have imposed purely toroidally polarised footpoint motions and that the arcade under consideration is a potential one (there is no electrical current in the equilibrium state present), we obtain

$$[\mathbf{E} \times \mathbf{B}^*]_{z=0} = -v_y b_y^* B_z, \tag{32}$$

where any term proportional to η is neglected because of the very high Reynolds numbers under solar coronal conditions (see e.g. Ruderman et al. 1997b). The z-component of the time averaged Poynting flux S can then be written as

$$S = -\frac{1}{2}\int_{-L}^{0} [Re(v_y b_y^* B_z)]_{z=0} \mathrm{d}x. \tag{33}$$

Expressing v_y and b_y in terms of the displacement component ξ_y results in

$$S = \frac{\omega}{2}\int_{-\pi/2}^{0} [Re(i\xi_y \frac{(1-\psi'^2)^{\frac{1}{2}}}{J} \frac{\partial \xi_y^*}{\partial \chi'} B_z)]_{z=0} \mathrm{d}x, \tag{34}$$

where we wrote S now in non-dimensionalised form.

Changing the integration variable to the flux coordinate ψ' we can rewrite expression (34) as

$$S = \frac{\omega}{2}\int_{0}^{1} Re(i\xi_y \frac{\partial \xi_y^*}{\partial \chi'}) \frac{\mathrm{d}\psi'}{J(1-\psi'^2)^{\frac{1}{2}}}|_{\chi'=-1}. \tag{35}$$

In terms of ϕ the expression for the averaged Poynting flux through the left foot of the arcade becomes

$$S = \frac{\omega}{2}\int_{0}^{1} R_y Im(\frac{\partial \phi}{\partial \chi'}) \frac{\mathrm{d}\psi'}{J(1-\psi'^2)^{\frac{1}{2}}}|_{\chi'=-1}. \tag{36}$$

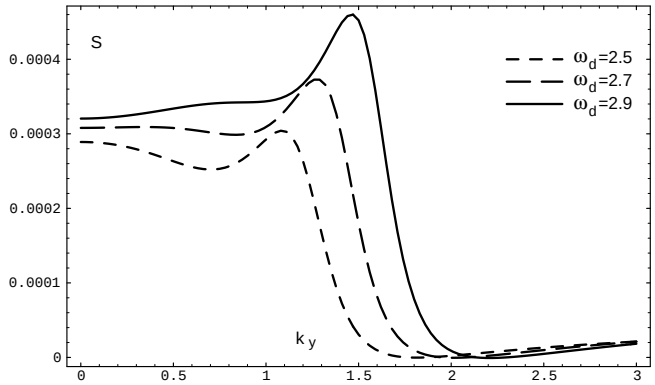

Fig. 3. The k_y-dependence of the time averaged Poynting flux S through the left foot of the arcade for $\omega_d = 2.5, 2.7, 2.9$ in the absence of a quasi-mode.

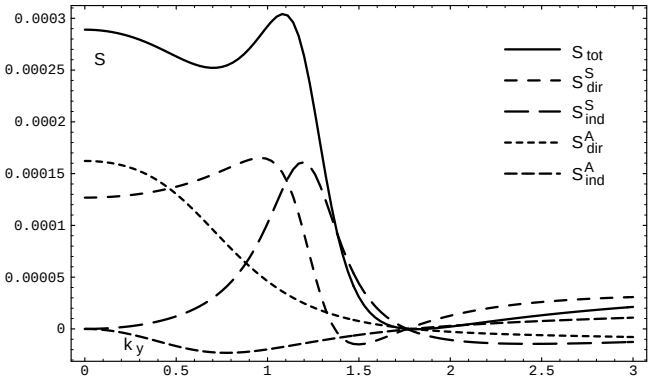

Fig. 4. The k_y-dependence of the time averaged Poynting flux S through the left foot of the arcade for $\omega_d = 2.5$ together with its direct and indirect components S^S_{dir}, S^A_{dir}, S^S_{ind} and S^A_{ind} in absence of a quasi-mode.

Since in a stationary state no energy stock can be built up in the arcade, S also equals the heating rate in the arcade. In addition, it will be interesting to examine also the Poynting flux which enters the resonant layer *directly* at its photospheric base, defined as

$$S_{dir} = \frac{\omega}{2} \int_{res.layer} R_y Im(\frac{\partial \phi}{\partial \chi'}) \frac{d\psi'}{J(1-\psi'^2)^{\frac{1}{2}}}|_{\chi'=-1}. \qquad (37)$$

When $k_y = 0$, S_{dir} equals the analytical expression for the total amount of dissipated wave energy derived by Ruderman et al. (1997b). The difference

$$S_{ind} = S - S_{dir} \qquad (38)$$

is the energy flux that enters the arcade through the left foot of the arcade at $z = 0$ plane, but outside the base of the resonant layer. Since only the dissipative layer can act as a sink of energy (by conversion to heat, of course), all the energy flux S_{ind} that goes to the non-resonant part of the arcade, has to leave it again which it can only do sideways into the dissipative layer. As such, S_{ind} is the energy flux entering the dissipative layer sideways and is referred to as the *indirect* energy flux. Of course, it is the coupling to the fast waves which is responsible for the indirect energy flux.

Note that the total energy flux S must be positive (since it equals the ohmic dissipation which is always a positive quantity), while the direct S_{dir} and the indirect S_{ind} energy flux can be negative (as long as their sum is positive).

6. Results and discussion

As already mentioned, since the arcade is symmetric with respect to $\chi = 0$, the eigenfunctions (for both the fast magnetosonic and the Alfvén spectrum) split up in a set of even functions and a set of odd functions. For the same reason, the solution of the footpoint driven problem can be found as the sum of a symmetric part (as an expansion in the even Alfvén eigenfunctions) and an antisymmetric part (as an expansion in the odd Alfvén eigenfunctions) which are decoupled.

As an instructive example to show the influence of the coupling to the fast waves and the presence of a quasi-mode on the resonant excitation of Alfvén waves, we will focus on driving frequencies in the range of $[2.1, 3.1]$. This means that both fundamental symmetric and antisymmetric Alfvén modes are excited on certain magnetic surfaces. In this range of frequencies the fundamental fast mode eigenfrequency is present (see Fig. 2). When $k_y \neq 0$, the fast mode resonantly couples to the fundamental symmetric Alfvén mode on the magnetic surface where the oscillation frequency matches the local Alfvén frequency (see Fig. 2). However, by shifting the boundaries in the ψ direction, we can control whether or not a quasi-mode is present in the considered range of driving frequencies. By shifting the boundaries inwards (the ψ-interval becomes smaller) the frequency of the fundamental fast mode increases and shifts out of the range of driving frequencies. Once the boundaries are specified, we are left with the two free parameters, ω_d and k_y, which determine the footpoint driving with the ψ-dependence described by $R_y(\psi)$. In the next subsection we first focus on the case without a quasi-mode lying in the discussed range of driving frequencies, while in the following subsection we look at the modifications induced by the presence of the fundamental quasi-mode. In each case we investigate the wave heating as a function of the footpoint parameters (ω_d, k_y). In the calculations we have taken η to be of the order 10^{-9} and R_y to be constant (and hence a scaling factor in our linear approach).

6.1. In the absence of a quasi-mode

We take the outer boundary $\psi_{out} = 0.2$ and the inner boundary of the arcade $\psi_{in} = 0.9$. For these rather artificial boundary values the fundamental fast mode frequency lies far above the considered range of driving frequencies $[2.5, 3.0]$.

In Fig. 3 we show the k_y-dependence of the averaged Poynting flux S through the left foot of the arcade for different driving frequencies. They all show the same global dependency : with increasing k_y there is an increase in time averaged Poynting flux leading to a maximum in Poynting flux (preceded by a lit-

tle decrease for smaller values of driving frequency), followed by a rather fast decay towards a point where the averaged energy input drops to zero. To investigate this in more detail we have plotted the total time averaged Poynting flux S together with the Poynting fluxes S^S_{dir} and S^A_{dir} through the photospheric base of the resonance layers in the symmetric part and the antisymmetric part of the solution, and their complements S^S_{ind} and S^A_{ind} for $\omega_d = 2.5$ in Fig. 4. This picture can be understood as follows. When $k_y = 0$ different magnetic surfaces are perfectly decoupled in ideal MHD, and the dissipative layer can only get energy input from its photospheric base resulting in $S = S^S_{dir} + S^A_{dir}$ and $S^S_{ind} = 0 = S^A_{ind}$. For $k_y \neq 0$ however, the magnetic surfaces are coupled and energy can now also enter or leave the dissipative layer sideways. As a consequence, S^S_{dir} and S^A_{dir} decay from a global point of view (wave energy is not perfectly contained in the dissipative layer anymore) and $|S^S_{ind}|$ and $|S^A_{ind}|$ grow (wave energy can enter or leave the dissipative layer sideways). For the antisymmetric part of the solution the sideways contribution S^A_{ind} remains small compared to S^A_{dir}. The contribution S^A_{ind} corresponds to 'fast wave' behaviour, since Alfvén waves propagate their energy strictly along the magnetic field. However 'antisymmetric fast mode' behaviour is not at all supported at the driving frequency $\omega_d = 2.5$. This results in a small S^A_{ind} contribution. For the symmetric part of the solution the sideways contribution S^S_{ind} becomes of the same order as S^S_{dir}. This is probably due to the presence of the fundamental symmetric quasi-mode with an nearby oscillation frequency $\omega \approx 3.7$, leading to an optimal coupling for $k_y \approx 1.1$. However for $k_y \approx 1.75$ all direct and indirect Poynting fluxes approach zero. In the (ω_d, k_y) space this results in an anti-resonance line of combination of driving frequency and wave number for which no resonance is built up. This feature was not encountered (or at least not mentioned) by Berghmans & Tirry (1997) in their investigation of wave heating in their 1-D coronal loop model.

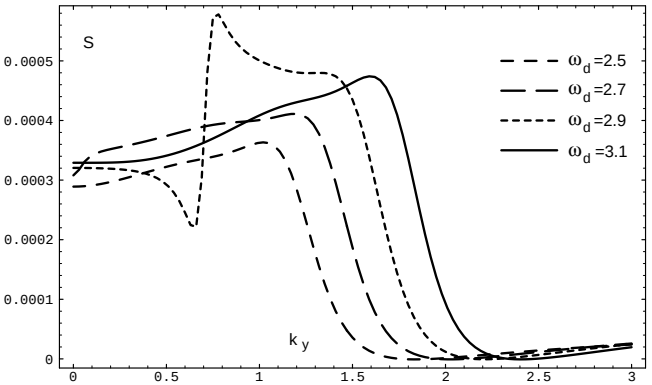

Fig. 5. The k_y-dependence of the time averaged Poynting flux S through the left foot of the arcade for $\omega_d = 2.5, 2.7, 2.9, 3.1$ in the presence of a quasi-mode.

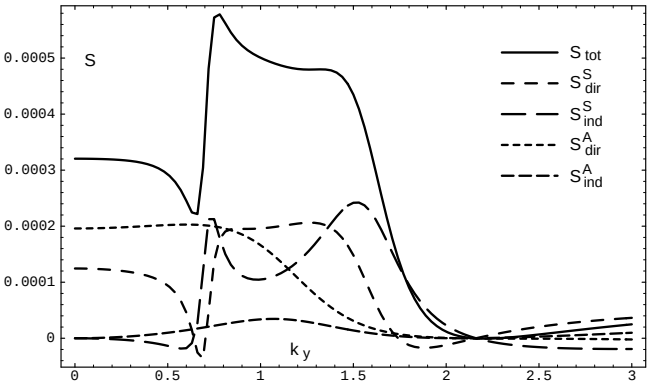

Fig. 6. The k_y-dependence of the time averaged Poynting flux S through the left foot of the arcade for $\omega_d = 2.9$ together with its direct and indirect components S^S_{dir}, S^A_{dir}, S^S_{ind} and S^A_{ind} in the presence of a quasi-mode.

6.2. In the presence of a quasi-mode

We now take the outer boundary $\psi_{out} = 0.03$ and the inner boundary $\psi_{in} = 0.97$. For these boundary values the fundamental fast mode frequency equals 2.71, lying in the considered range of driving frequencies. In Fig. 5 we show again the k_y-dependence of the time averaged Poynting flux S through the left foot of the arcade for different driving frequencies. From a global point of view, we could say that the dependence on k_y of the Poynting flux S remains the same as in the previous subsection with the same features : with increasing k_y, an optimal combination of driving frequency and wave number followed by an anti-resonance combination for which there is no time averaged photospheric energy input.

However, in the neighbourhood (in (ω_d, k_y) space) of the fundamental fast mode frequency, the appearance of the Poynting flux S changes dramatically. This can be seen clearly in Fig. 5 for $\omega_d = 2.9$ and $k_y \approx 0.77$. For small values of k_y the oscillation frequency of the fundamental quasi mode approaches the fundamental fast mode frequency. However for these small values of k_y, the coupling is very weak, so that the presence of the quasi-mode has almost no influence on the curve for $\omega_d = 2.7$ in Fig. 5. As discussed in the paper by Berghmans & Tirry (1997), the (ω_d, k_y) values of enhanced Poynting fluxes correspond to the position of the fundamental quasi-mode frequency (we refer by quasi-mode frequency actually to the real part of the quasi-mode frequency. The imaginary part (damping rate) is less important in the present discussion). Berghmans & Tirry also found a 'valley' of combinations of ω_d and k_y for which the footpoint driving leads to only a very small Poynting flux S, with a line in the middle of the valley where the Poynting flux S drops to zero. Although we recover a small valley of reduced Poynting flux, no anti-resonance is present therein (see Fig. 5 for $\omega_d = 2.9$). The reason is quite obvious and will be explained with Fig. 6. In Fig. 6 we have drawn as in Fig. 4 the total time averaged Poynting flux together with the fluxes S^S_{dir} and S^A_{dir} through the photospheric base of the resonance layers and their complements S^S_{ind} and S^A_{ind} for $\omega_d = 2.9$. Here we see that S^A_{dir} and S^A_{ind} corresponding to the antisymmetric part of the solution behave like in the case of absence of a quasi-mode. The antisymmetric behaviour does not feel the

presence of the symmetric fundamental quasi-mode. However the symmetric part of the stationary state solution does. In the neighbourhood (in (ω_d, k_y) space) of the fundamental quasi-mode frequency the appearance of the Poynting fluxes S^S_{dir} and S^S_{ind} is in agreement with the behaviour found by Berghmans & Tirry : with increasing k_y, an anti-resonance point (both S^S_{dir} and S^S_{ind} goes through zero) followed by an enhanced Poynting flux region. The anti-resonance line can be explained in terms of being those (ω_d, k_y) combinations for which the resonant Alfvén waves excited directly at the photospheric base of the dissipative layer are in perfect anti-phase with the Alfvén waves excited through coupling with the fast waves. The region of enhanced Poynting flux corresponds to combinations for which the contributions are almost in phase. This was shown by Tirry & Berghmans (1997) in their time-dependent approach of the photospheric excitation of Alfvén waves in a 1-D coronal loop.

Hence our results for the photospheric excitation of Alfvén waves in a potential coronal arcade confirm the peculiar behaviour found by Berghmans & Tirry that a region (in (ω_d, k_y) space) of enhanced Poynting flux due to the presence of a quasi-mode is accompanied with a region of reduced Poynting flux.

7. Summary

In this paper we investigated the excitation of resonant Alfvén waves in coronal arcades by toroidally polarised motions of the photospheric footpoints of the fieldlines.

Our main interest was to obtain qualitative information on the new wave physics due to the toroidal wave number $k_y \neq 0$ and to confirm the peculiar phenomenon of anti-resonance previous encountered by Berghmans & Tirry (1997).

We considered a potential coronal arcade of a pressureless plasma obeying the linear resistive MHD equations. We were able to determine analytically the 2-D solution in the dissipative layer around the resonant magnetic surface, where the driving frequency equals the local Alfvén frequency. Hence the only numerical effort to find the wave solution in the stationary state lay in the integration of the ideal MHD equation away from any singularity. Since this saves a lot of memory and CPU time, parametric studies can easily be done.

In addition, we derived expressions for the energy fluxes entering the dissipative layers through its photospheric base and the energy fluxes entering the dissipative layers sideways. The sum of these fluxes is the total energy flux delivered by the footpoint motions and dissipated in the coronal arcade. These expressions turned out to be valuable tools for the investigation of the stationary heating of the coronal arcade as a function of the footpoint characteristics (ω_d, k_y).

For $k_y = 0$, as studied by Ruderman et al. (1997b), there is no coupling to fast waves and thus the only way for the resonance layer to obtain energy is by direct input from its photospheric base. In order to investigate the influence of the presence of a quasi-mode, we first studied the case in absence of a quasi-mode. When $k_y \neq 0$ the different magnetic surfaces are coupled. Hence the energy is now not only entering (or leaving) the dissipative layer from below but also sideways with a combination of ω_d and k_y leading to optimal heating rate. However in contrast to Berghmans & Tirry, there is also a combination of ω_d and k_y where both the direct Poynting fluxes S^S_{dir} and S^A_{dir} and as the indirect fluxes S^S_{ind} and S^A_{ind} go through zero, leading to virtually no heating at all.

In the case of presence of a quasi-mode the dependence of the heating on the driving frequency and the wave number is drastically changed. For (ω_d, k_y) corresponding to the quasi-mode, the heating rate is enhanced, however not by several orders of magnitude as Berghmans & Tirry found in their 1-D coronal loop model. The associated region in (ω_d, k_y) space of reduced Poynting flux S is also recovered. However, no line of anti-resonance is present therein. The reason is that the resonance of the antisymmetric fundamental Alfvén eigenmode is not influenced by the presence of the symmetric fundamental quasi-mode. When considering only the direct and indirect Poynting fluxes corresponding to the symmetric part of the solution, the anti-resonance is recovered.

Hence our results for the photospheric excitation of Alfvén waves in a potential coronal arcade confirm the peculiar behaviour found by Berghmans & Tirry that a region (in (ω_d, k_y) space) of enhanced Poynting flux due to the presence of a quasi-mode is accompanied with a region of reduced Poynting flux.

Acknowledgements. The authors are grateful to M. Goossens for his suggestion to undertake this work. They also gratefully acknowledge the valuable discussions with D. Berghmans.

References

Acton, L., Tsuneta, S., Ogawara, R. et al., 1992, Sci, 258, 618
Berghmans, D., & De Bruyne, P. 1995, ApJ, 453, 495
Berghmans, D., & Tirry, W.J. 1997, A&A, in press
Boris, J.P. 1968, 'Resistive modified normal modes of an inhomogeneous incompressible plasma', Ph.D. Thesis Princeton University
Čadež, V.M., & Ballester, J.L. 1995a, A&A, 296, 537
Čadež, V.M., & Ballester, J.L. 1995b, A&A, 296, 550
Čadež, V.M., & Ballester, J.L. 1996, A&A, 305, 977
Falconer, D.A., Moore, R.L., Porter, J.G., Gary, G.A., & Shimizu, T. 1996, ApJ, 482, 519
Goossens, M., Ruderman, M.S., & Hollweg, J.V. 1995, SPh, 157, 75
Heyvaerts, J., & Priest, E.R. 1983, A&A, 117, 220
Hollweg, J.V. 1984, ApJ, 277, 392
McAllister, A., Uchida, Y., Tsuneta, S. et al., 1992, PASJ, 44, L205
Oliver, R., Ballester, J.L., Hood, A.W., & Priest, E.R. 1993, A&A, 273, 647
Oliver, R., Hood, A.W., & Priest, E.R. 1996, ApJ, 461, 424
Parker, E.N. 1972, ApJ, 174, 499
Pasachoff, J.M., & Landman, D.A. 1984, SPh, 90, 325
Pasachoff, J.M., & Ladd, E.F. 1987, SPh, 109, 365
Pasachoff, J.M. 1991, in: Ulmschneider P., Priest E.R., Rosner R. (eds.) Mechanisms of Chromospheric and Coronal Heating, Springer, Berlin, 25
Poedts, S., & Goossens, M. 1991, SPh, 133, 281
Poedts, S. & Boynton, G.C. 1996, A&A, 306, 610
Ruderman, M.S., Berghmans, D., Goossens, M., & Poedts, S. 1997a, A&A, 320, 305
Ruderman, M.S., Goossens, M., Ballester, J.L., & Oliver, R. 1997b A&A, accepted

Saba, J., & Strong, K. 1991, ApJ, 375, 789
Smith, J.M., Roberts, B., & Oliver, R. 1997, A&A, 317, 752
Tirry, W.J., & Goossens M. 1996, ApJ, 471, 501
Tirry, W.J., & Berghmans, D. 1997, A&A, in press
Tsubaki, T. 1988, in Solar and Stellar Coronal Structures and Dynamics, ed. Altrock, R.C.,140
Van Ballegooijen, A.A. 1985, ApJ, 298, 421
Watari, S., Detman, T., & Joselyn, J.A. 1996, SPh, 169, 167
Weiss, L.A., Gosling, J.T., McAllister, A.H. et al., 1996, A&A, 316, 384
Zirker, J.B. 1993, SPh, 148, 43

This article was processed by the author using Springer-Verlag LaTeX A&A style file *L-AA* version 3.